DOI: 10.1002/ejoc.200800973

Indenylidene Complexes of Ruthenium Bearing NHC Ligands – Structure Elucidation and Performance as Catalysts for Olefin Metathesis

Stijn Monsaert,[a] Els De Canck,[a] Renata Drozdzak,[a] Pascal Van Der Voort,[a] Francis Verpoort,*[a] José C. Martins,*[b] and Pieter M. S. Hendrickx[b]

Keywords: Ruthenium / Olefin metathesis / Conformation analysis / Homogeneous catalysis / Indenylidene

Second-generation catalysts of the general formula Cl_2Ru(SIMes)(L)(3-phenylinden-1-ylidene), **3a** (L = PCy_3), **3b** (L = PPh_3), **3c** (L = py), and Cl_2Ru(SIMe)(L)(3-phenylinden-1-ylidene), **4a** (L = PCy_3), **4b** (L = PPh_3), **4c** (L = py) were found to be of interest in various metathesis transformations. The catalysts containing SIMe ligands showed improved initiation compared to the more robust SIMes substituted catalysts. A strong temperature effect was noted on all of the reactions tested. Interestingly, complex **3a**, showing the lowest initiation rate at room temperature, emerged as the most productive of all systems examined at elevated temperature. It is shown that complexes containing the SIMe ligand display higher initiation efficiency than their corresponding SIMes analogues. Since the higher initiation is related to the ease of phosphane dissociation while phosphane dissociation also promotes catalyst decomposition, complexes bearing the SIMe ligand decompose faster. The complete ^1H, ^{13}C and ^{31}P resonance assignment and the procedure applied to obtain these from a combination of 1D and 2D NMR techniques, is also reported. Combined with the ROESY technique, these enabled to investigate several conformational processes involving rotations around *N*–phenyl and C–Ru bonds on the millisecond to second timescale. A clear correlation is demonstrated between the bulkiness of the axial ligand (L) and the rotational freedom of the SIMe(s) ligand. A qualitative analysis also suggests that the extra *para*-methyl of SIMes leads to additional steric interactions with the 3-phenylinden-1-ylidene ligand. The data reported in this paper demonstrates that substitution patterns of the *N*-aryl have a significant influence on the activity of the second-generation indenylidene catalysts for a given metathesis reaction.

Introduction

The appearance of well-defined ruthenium-based precatalysts for metathesis has prompted an unusual growth of interest in this transformation both from the fine chemical and polymer industry.[1a–1d] In particular, the neutral ruthenium carbene complex **1a** developed by Grubbs and coworkers turned out to be exceedingly useful, combining a high catalytic activity with a good to excellent tolerance towards polar functional groups.[2a,2b] Among the numerous variations on the ligand sphere of **1a**, the replacement of one phosphane ligand by a *N*-heterocyclic carbene moiety was found to impart a significant increase in activity as well as stability in solution.[2c–2i] Another important milestone on the metathesis road of success was the introduction of chelating ligands by Hoveyda,[3a,3b] Grela[4a,4b] and Blechert,[5a–5c] leading to catalysts that display excellent reactivities toward electron-deficient substrates.

Although the rapidly increasing demand for metathesis catalysts has led to the development of highly active ruthenium precatalysts for advanced synthetic tasks, a search for commercially relevant, alternative metathesis initiators of comparable performance to Grubbs' catalysts and improved accessibility remains challenging. In this context, the ruthenium indenylidene complex **2a**, has been introduced and described as a particularly well suited precatalyst for cyclization of medium-sized rings by Ring-Closing Metathesis (RCM) reactions (Figure 1).[6–8]

The incorporation of NHC ligands led to complexes **2c** and **3a** in which there is a pronounced decrease in the initiation rate compared to **2a**. This drawback is offset, however, by their increased thermal stability, which is beneficial for many Ring-Closing Metathesis reactions performed at elevated temperatures.[6,8] Even though the indenylidene catalysts appeared to be very attractive from a practical point of view, as they can be very easily prepared from commercially available precursors,[7] the structure and substantial variations of its basic structural motif have not been well explored. In the following we summarize our investigations in this field. In an attempt to expand the application profile

[a] Department of Inorganic and Physical Chemistry, Ghent University,
Krijgslaan 281 (S3), 9000 Ghent, Belgium
Fax: +32-9-264-4183
E-mail: Francis.Verpoort@UGent.be
[b] Department of Organic Chemistry, Ghent University,
Krijgslaan 281 (S4), 9000 Ghent, Belgium
Fax: +32-9-264-4972
E-mail: Jose.Martins@UGent.be

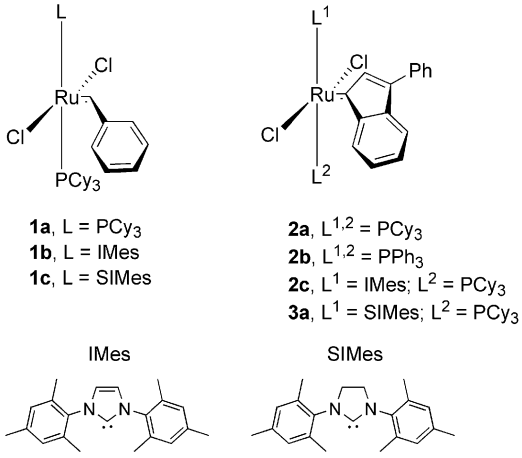

Figure 1. Benzylidene and indenylidene ruthenium complexes.

of indenylidene catalysts, we have investigated the effects of changing the substitution patterns in the aryl groups of the NHC on the catalytic activity of the corresponding ruthenium complexes. Recently Schrodi et al. described that removing the methyl substituents in *ortho*- and *para*-position of the *N*-aryl ring led to a large increase in reactivity of Grubbs' catalyst **1c**.[9] Following this lead, catalysts in which the NHC ligands only bear *ortho*-methyl substituents (SIMe) **4a**–**c** were prepared and compared to **3a**–**c** bearing both *ortho*- and *para*-methyl substituents.

The series of indenylidene complexes prepared in this study were fully characterised using NMR spectroscopy. This was motivated by the fact that little information is available on the solution behaviour of such complexes. In addition, the chemical shift is very sensitive to both conformational and subtle stereo electronic effects. Therefore, provided such NMR spectroscopic data is obtained from a sufficiently large collection of complexes, correlations with the catalytic activity may ultimately be inferred from analysis of the NMR spectroscopic data. Here, a general route to and complete NMR characterization of the complexes **3a**–**c**, **4a**–**c** is presented, with full ^{1}H, ^{13}C and ^{31}P assignment and an investigation of the dynamics of rotameric processes occurring from hindered rotation along a variety of bonds.

The activity of this new class of indenylidene catalysts **4a**–**c** with respect to the analogous family **3a**–**c** and Grubbs' catalysts **1c**, was determined by establishing their performance in catalysing different reaction types. More specifically, Ring-Closing Metathesis (RCM) of dienes, alkene Cross-Metathesis (CM) and Ring-Opening Metathesis Polymerization (ROMP) have been evaluated.

Results and Discussion

Synthesis of Indenylidene-Ru Complexes 3a–c and 4a–c

A most attractive feature of neutral indenylidene complexes such as **2a** and **2b** stems from the ease of formation of the Ru=C bond of the indenylidene moiety, which is achieved by reaction of $Ru(Cl)_2(PPh_3)_{3-4}$ with a propargyl alcohol.[7] It has been recently described by our group, that the most suitable method for converting **2a** into its 2nd-generation analogues, appears to be the "one-pot" thermal decomposition of specific adducts[6] such as the chloroform adduct **5a** or pentafluorobenzene adduct **5b** (Figure 2). These methods give access to a set of structurally diverse indenylidene ruthenium complexes by variation of the labile ligands as well as the NHC ligands.

Reaction progress was easily followed by ^{31}P NMR through the appearance of a new, upfield peak (δ = 27.0 ppm and 26.1 ppm for **3a** and **4a**, respectively, vs. δ = 33.5 ppm for the starting complex **2a**). Complete conversion was observed within 1.5 h. Complexes **3a** and **4a**, red powders after precipitation in methanol, were isolated in high yields. The synthesis of **3c** and **4c** proceeded easily by treat-

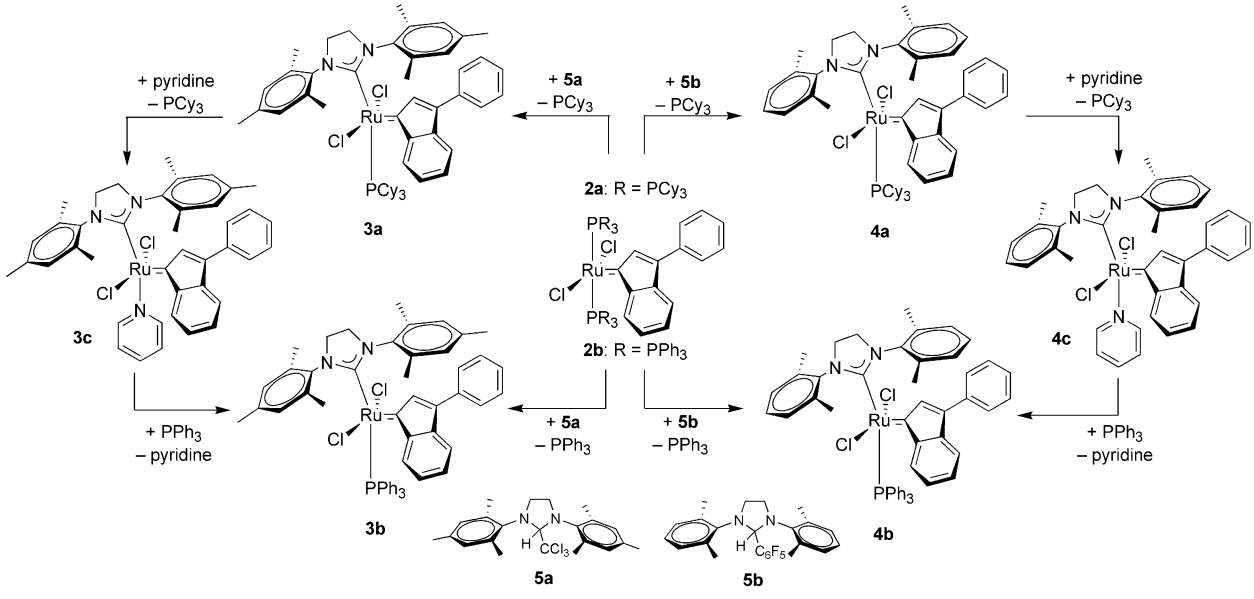

Figure 2. Synthetic pathways to 2nd- and 3rd-generation indenylidene-Ru metathesis catalysts.

ment with an excess of pyridine.[2e,10] The indenylidene complexes **3c** and **4c**, precipitated from the reaction mixture with hexane at –40 °C, were washed several times with small portions of hexane, and recrystallized from CH_2Cl_2/hexane to yield orange-brown solids (η = 70% for **3c** and 60% for **4c**) that were fully characterized spectroscopically. Complexes **3b** and **4b** were obtained from **3c** and **4c** by simple ligand exchange and isolated as clear red powders. In addition, they were straightforwardly obtained from reaction of **2b** with **5**.

Structural Analysis of Complexes 3a–c and 4a–c

In order to fully characterize this set of compounds, a series of 1D ^1H and ^{13}C spectra complemented by 2D spectra consisting of homonuclear ^1H-{^1H} COSY, TOCSY, NOESY and heteronuclear ^1H-{^{13}C} HSQC and HMBC spectra, was used. The complete ^1H and ^{13}C resonance assignment of the common ligands is collected in Table 1 while Tables 2, 3, and 4 hold the assignments of the variable ligand.

Table 2. ^1H, ^{13}C and ^{31}P assignments of the PCy_3 ligand in **3a** and **4a**.[a]

Atom label	**3a** $^1H_{ax}$	**3a** $^1H_{eq}$	**3a** ^{13}C	**4a** $^1H_{ax}$	**4a** $^1H_{eq}$	**4a** ^{13}C
35	2.45	–	33.0	2.45	–	33.0
36/40	1.22	1.84	29.5	1.20	1.82	29.4
36/40	1.18	1.72	29.4	1.14	1.67	29.3
37/39	1.10	1.59	27.8	1.11	1.60	27.9
37/39	1.09	1.53	27.7	1.09	1.53	27.8
38	1.06	1.52	26.2	1.09	1.51	26.3
^{31}P	27.0			26.1		

[a] Arbitrary numbering is depicted in Figure 3. Chemical shifts are quoted in ppm with respect to residual C_6D_5H as secondary internal reference. Assignments are partly based on chemical shift predictions. The measurement conditions are the same as in Table 1.

Table 1. ^1H and ^{13}C assignments of the NHC and indenylidene moieties common to compounds **3a**–**c** and **4a**–**c** at 298 K in [D_6]benzene solution.[a]

Atom label	**3a** ^1H	**3a** ^{13}C	**3b** ^1H	**3b** ^{13}C	**3c** ^1H	**3c** ^{13}C	**4a** ^1H	**4a** ^{13}C	**4b** ^1H	**4b** ^{13}C	**4c** ^1H	**4c** ^{13}C
1	–	135.6	–	136.7	–	134.3	–	138.0	–	138.0	–	136.9
2	–	139.0	–	140.2	–	140.8	–	139.4	–	139.6	–	141.1
3	6.96	130.0	6.93	131.0	6.96	129.6	7.14	128.9	≈ 7.15	129.0	7.16	128.9
4	–	136.6	–	138.8	–	138.5	7.10	128.9	≈ 7.15	128.9	6.53	128.4
5	6.96	130.0	6.91	131.0	7.03	129.2	7.14	128.9	≈ 7.15	128.9	7.20	128.4
6	–	139.0	–	140.4	–	140.4	–	139.6	–	139.7	–	140.5
Me7	2.85	20.3	2.82	21.6	2.75	21.0	2.82	20.5	2.79	20.5	2.74	20.9
Me8	2.87	20.3	2.84	21.5	3.02	21.2	2.87	20.5	2.87	20.5	3.04	21.2
Me9	2.23	20.9	2.26	22.0	2.16	20.7	–	–	–	–	–	–
10a	3.37	52.1	6.42	52.8	3.45	50.2	3.28	51.7	3.30	51.4	3.38	50.0
10b	3.37	52.1	6.42	52.8	3.58	50.2	3.30	51.7	3.30	51.4	3.50	50.0
11a	3.26	51.6	6.25	52.6	3.22	51.8	3.08	51.5	3.09	51.3	3.13	51.5
11b	3.17	51.6	3.17	52.6	3.37	51.8	3.17	51.5	3.16	51.3	3.31	51.5
12	–	136.8	–	137.9	–	136.3	–	139.0	–	138.8	–	138.3
13	–	136.8	–	137.9	–	136.9	–	137.0	–	137.1	–	137.5
14	6.47	129.2	6.43	130.2	6.41	129.2	6.62	128.2	6.56	128.3	7.20	128.4
15	–	136.6	–	137.7	–	137.3	6.54	128.2	6.56	128.3	6.53	128.4
16	6.02	128.6	6.07	130.0	6.28	129.3	6.28	127.7	6.30	128.0	7.16	127.9
17	–	137.6	–	137.6	–	136.8	–	136.8	–	136.9	–	137.5
Me18	2.22	18.7	2.15	19.8	2.02	18.2	2.23	18.9	2.13	18.6	2.04	18.4
Me19	2.38	18.5	2.31	19.6	2.50	18.5	2.39	18.7	2.33	18.7	2.51	18.5
Me20	1.80	20.7	1.82	21.8	1.73	20.7	–	–	–	–	–	–
21	–	217.3	–	216.8	–	215.2	–	≈ 215	–	≈ 215	–	214.8
22	–	292.2	–	300.9	–	300.4	–	293.1	–	300.7	–	301.3
23	7.84	137.8	7.10	139.1	7.22	139.3	7.76	138.0	7.01	138.1	7.11	139.6
24	–	138.0	–	141.2	–	139.2	–	137.3	–	140.6	–	139.6
25	–	145.0	–	144.5	–	143.4	–	145.2	–	143.4	–	143.2
26	7.08	116.0	6.96	117.2	7.11	116.5	7.07	116.5	6.96	116.4	7.07	116.7
27	7.11	126.8	7.04	128.8	7.07	128.5	7.12	127.2	6.88	127.4	7.03	128.7
28	7.18	128.2	6.90	128.4	7.03	128.6	7.19	128.1	7.05	127.8	7.00	129.2
29	9.15	129.5	8.39	130.2	9.08	128.4	9.20	129.6	8.35	129.2	9.06	128.3
30	–	141.2	–	142.4	–	141.2	–	141.4	–	141.6	–	141.3
31	–	136.0	–	137.9	–	137.2	–	136.7	–	136.9	–	137.2
32	7.89	126.2	7.63	127.5	7.82	126.4	7.86	126.5	7.62	126.5	7.80	126.5
33	7.25	128.9	7.20	129.9	7.14	128.9	7.23	129.0	7.19	128.7	7.15	128.7
34	7.32	127.3	7.33	128.7	7.30	127.5	7.30	127.3	7.32	127.6	7.31	127.5

[a] The arbitrary numbering is depicted in Figure 3. Chemical shifts are quoted in ppm with respect to residual C_6D_5H as secondary internal reference. The dividing horizontal line separates the assignments of the SIMe(s) *N*-heterocyclic carbene ligand C from those of the indenylidene group.

Table 3. ^{1}H and ^{13}C assignments of the pyridine ligand in **3c** and **4c**.[a]

Atom label	**3c** ^{1}H	**3c** ^{13}C	**4c** ^{1}H	**4c** ^{13}C
35	8.18	152.9	8.51	150.8
36	6.09	123.7	6.07	123.8
37	6.37	136.8	6.35	136.8

[a] Arbitrary numbering is depicted in Figure 3. Chemical shifts are quoted in ppm with respect to residual C_6D_5H as secondary internal reference. The measurement conditions are the same as in Table 1.

Table 4. ^{1}H, ^{13}C and ^{31}P assignments of the PPh_3 ligand in **3b** and **4b**.[a]

Atom label	**3b** ^{1}H	**3b** ^{13}C	**4b** ^{1}H	**4b** ^{13}C
35	–	135.5	–	132.9
36	7.45	135.5	7.45	135.6
37	6.91	130.8	6.92	129.8
38	6.97	129.8	6.96	129.9
^{31}P	27.3		27.5	

Arbitrary numbering is depicted in Figure 3. Chemical shifts are quoted in ppm with respect to residual C_6D_5H as secondary internal reference. The measurement conditions are the same as in Table 1.

In the following, only the spectral assignment of **3a** will be described in detail, all other compounds being characterized in a similar fashion. The arbitrary numbering, as depicted in Figure 3, will be used throughout.

As an unambiguous starting point of the assignment, the six methyl ^{1}H resonances of the SIMes ligand, which occur as sharp singlets in the aliphatic spectral region, were chosen. The resonances of their attached carbon atoms were obtained from the HSQC spectrum. The aromatic protons of the SIMes ligand (H^3, H^5, H^{14} and H^{16}) could then be identified using a combination of nOe and $^nJ_{CH}$ correlations to the methyl groups. This also afforded to group individual methyl and aromatic ^{1}H and ^{13}C resonances to each of the mesitylene ring moieties. Methyl to methyl nOe correlations involving H^7–H^{18} and H^8–H^{19} allowed to determine the relative position of these methyl groups and their associated aromatic ring with respect to each other, as shown in Figure 3.

Furthermore, strong nOe contacts, which correlate the *ortho*-methyl groups to four protons in the 3.10–3.40 ppm range, were also present. As these latter protons are pair wise correlated to carbon atoms resonating at δ = 52.1 and 51.6 ppm in the HSQC spectrum and show strong mutual nOe and TOCSY contacts, they could be unambiguously assigned to the SIMes bridgehead protons (H^{10} and H^{11}). HMBC correlations to a carbon resonance at δ = 217.3 ppm allowed identifying the carbene carbon atom (C^{21}) which is expected to resonate at high frequency.

As for the assignment of the indenylidene ligand, the C^{22} carbene at δ = 292.7 ppm is chosen as a starting point because of its conspicuous low-field frequency. As only two $^nJ_{CH}$ correlations to the carbene were found in the HMBC spectrum, H^{23} and H^{29} could be identified; they could be differentiated on the basis of their ^{1}H multiplicity (singlet vs. doublet). Further correlations in TOCSY, NOESY and HMBC spectra lead to the complete assignment of the H^{26}–H^{29} spin system as well as the quaternary carbon atoms of the main aromatic ring system. The H^{32}–H^{34} spin system from the phenyl moiety was identified using both TOCSY and HSQC spectra and was linked to the main ring by nOe and $^nJ_{CH}$ correlations. As the *ortho*- and *meta*-protons in the phenyl ring are isochronous, it can be concluded that the rotation around the C^{24}–C^{31} bond is fast on the NMR time scale.

Since the six methyl groups of the SIMes phenyls experience different magnetic environments, interpretation of their nOe contacts is greatly facilitated. Multiple nOe contacts connecting the SIMes methyl groups Me^{18}–Me^{20} with many indenylidene protons together with the absence of such contacts involving Me^7–Me^9, allows to position the phenyl ring with the higher numbering over the indenylidene ligand (Figure 3).

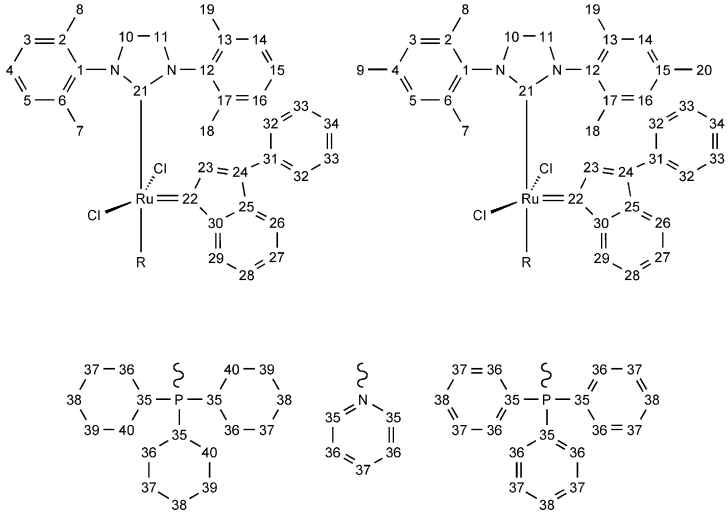

Figure 3. Arbitrary numbering of the common ligands of compounds **3a**–**c** (top, left) and **4a**–**c** (top, right) and of the variable ligand of compounds **3a** and **4a** (bottom, left), **3c** and **4c** (bottom middle) and **3b** and **4b** (bottom right).

In both complexes **3a** and **4a**, the tricyclohexylphosphane ligand shows one set of broad resonances in the 1D proton spectrum that sharpen somewhat as temperature is increased. This is explained by assuming non-equivalent environments for the cyclohexyl moieties in the ligand that interconvert through rotation around the Ru–P and P–C^{35} bonds in an intermediate to fast exchange regime. The assignment of all ^{1}H and ^{13}C resonances (Table 2) was validated by means of characteristic nOe contacts or through confrontation with predicted chemical shift values (ChemDraw 7.0, Cambridge Soft).

In the complexes bearing triphenylphosphane ligands (**3b** and **4b**) only one set of resonances is observed for this ligand, thus the rotation around the Ru–P bond must be fast on the NMR timescale. Furthermore, *ortho*- and *meta*-protons are again isochronous due to fast rotations around all P–C^{35} bonds. Resonance frequencies were obtained from HSQC and TOCSY spectra. Assignments were based on COSY correlations, signal intensity and multiplicity.

The pyridine ligand in complex **3c** and **4c** shows sharp resonances in the aromatic region. Its resonance frequencies were obtained from the HSQC and TOCSY spectra. Assignments were based on COSY correlations, signal intensity and multiplicity. As *ortho*- and *meta*-protons are yet again isochronous, it can be concluded that the rotation around the Ru–N bond is fast on the NMR time scale. The ^{1}H and ^{13}C NMR spectra clearly indicate coordination of only one pyridine,[6] in contrast to Grubbs's[2e,10a] and Nolan's[10b] complexes incorporating two pyridines.

A further characterization of the dynamical properties of complexes **3a**–**c** and **4a**–**c** was obtained by recording ROESY spectra using an off-resonance spin-locking scheme,[11] allowing to unambiguously distinguish nOe and exchange cross-peaks (Figure 4). Such exchange cross-peaks, due to rotations around the Ru–C^{21}, N–C^{1} and N–C^{12} bonds in the SIMes and SIMe ligand, could be observed for some complexes and are summarized in Table 5. It should be noticed that individual ring flips, i.e. rotations around the N–$C^{1/12}$ bonds, are only observed in complexes bearing pyridine. This can be explained as a steric effect when considering the size of the ligands. As PPh_3 and PCy_3 are bulky ligands, the indenylidene and chlorine ligand will be in closer contact with the NHC ligands and considerably hamper the phenyl ring flipping. Thus, a larger axial ligand opposite Ru will inhibit ring flipping. A hindered rotational motion around the Ru–C^{21} bond, in which the phenyl rings swap places, is observed in all complexes except for **3a**. The exchange peaks in **3b** being close to the detection limit already, we assume that the kinetics for this process in **3a** is too slow to yield detectable exchange peaks. While no quantitative processing was attempted, two trends are noteworthy.

First, under identical measuring conditions larger exchange cross-peaks are observed for the SIMe swapping than for the SIMes swapping process. This is tentatively interpreted as the result of an additional steric hindrance between the indenylidene phenyl ring and the *para*-methylgroups in SIMes. Also, exchange cross-peaks that can

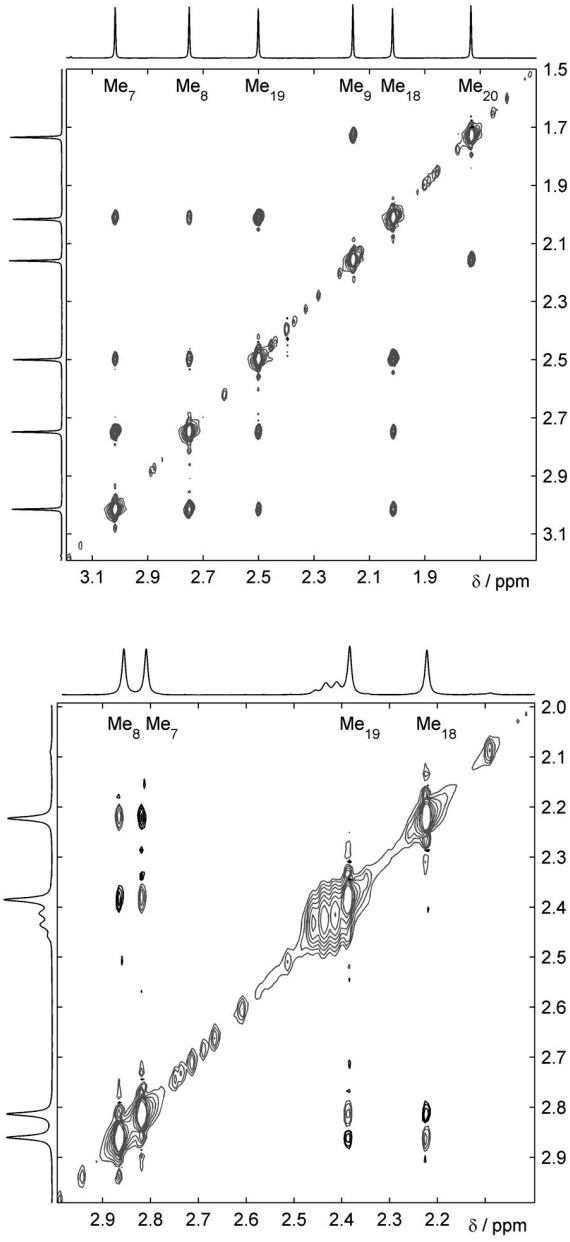

Figure 4. Detail of the 200 ms off-resonance ROESY spectrum demonstrating exchange cross-peaks (grey) indicative of hindered rotations that are slow on the NMR time scale around all possible SIMes bonds in compound **3c** (top) while a hindered rotation around the Ru–N(SIMe) bond only is observed in compound **4c** (bottom). Here, black cross-peaks indicate genuine nOe correlations (Me^{7}–Me^{18}; Me^{8}–Me^{19}) between methyl groups on both sides of SIMe.

Table 5. Qualitative overview of hindered rotations in compounds **3a**–**c** and **4a**–**c**.[a]

Bond	3a	3b	3c	4a	4b	4c
Ring flip N–$C^{1/12}$	–	–	+	–	–	+
Ring swap Ru–C^{21}	–	+	+	+	+	+

[a] Hindered rotations which are observed in off-resonance ROESY spectra are indicated with a (+) sign, unobserved rotations are indicated using a (–) sign.

only arise through a consecutive ring flip and swapping operation appear weaker than those resulting from a single flip or swap exchange peak, indicating that they occur independently from one another.

The indenylidene moiety is the only ligand that is consistently present in all complexes; therefore analysis of it's ^{1}H and ^{13}C chemical shifts can reveal similarities and differences as a function of the various ligands. For most protons and carbons, the chemical shift is not significantly affected by the presence or absence of the *para*-methyl in the SIMes and SIMe ligands, the chemical shifts of **3a**, **3b** and **3c** being almost identical to those seen in **4a**, **4b** and **4c** respectively. Keeping the NHC ligand fixed, some difference can be seen depending on the type of ligand L. Most notably, the chemical shift of H^{23} and the nearby carbene C^{22} of the indenylidene in **3a** and **3b**, differ by more than 0.5 and 8 ppm respectively, while these are quite similar in the other complexes. On the other hand, H^{29} is shifted 0.6 ppm to higher field in **3b** and **4b**, with respect to the other complexes. At the level of the SIMe/SIMes ligand, changes in the ^{1}H chemical shifts are clearly apparent when L is a pyridine as opposed to a PCy_3 or PPh_3. Since the ^{1}H chemical shifts of the PCy_3 and PPh_3 bearing complexes are quite similar, this is believed to reflect changes in the relative orientation of the various ligands in **3c** and **4c** concomitant with the considerably lower steric bulk of the pyridine ligand.

Metathesis Activity

A standard set of metathesis reactions[11] (see Schemes 1, 2, Table 7) and a more challenging one involving diphenyl diallylsilane (**10**) were used to depict the performance of complexes **3a**–**c** and **4a**–**c**.

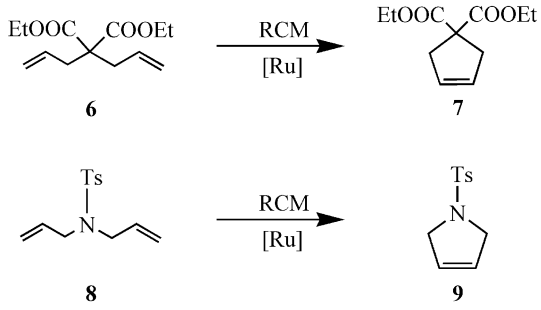

Scheme 1. Representative Ring-Closing Metathesis reactions.

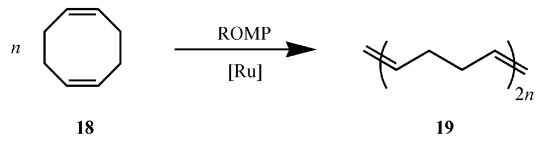

Scheme 2. ROM polymerization of 1,5-cyclooctadiene (COD) (**18**).

The RCM reaction of diethyl diallylmalonate **6** and *N*,*N*-diallyltosylamide **8** were selected for a first assay given their importance in synthetic chemistry[8] and the fact that they hold as general benchmark reactions for RCM reactions (Scheme 1 and Figures 5, 6, and 7).

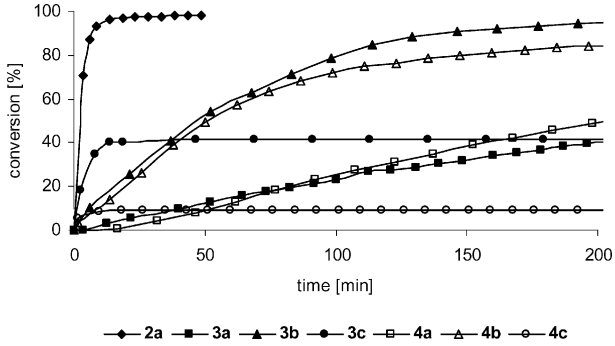

Figure 5. RCM of diethyl diallylmalonate (**6**), catalysts **3a**–**c**, **4a**–**c** and **2a**. Catalyst/substrate ratio 1:200; solvent: $CDCl_3$; temperature: 20 °C; conversion determined by ^{1}H NMR; lines are intended as visual aids only.

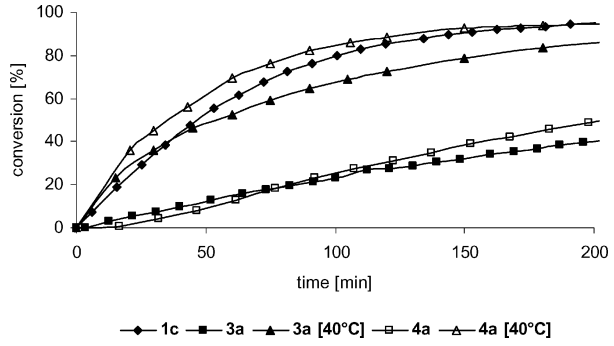

Figure 6. RCM of diethyl diallylmalonate (**6**), catalysts **1c**, **3a** and **4a**. Catalyst/substrate ratio 1:200; solvent: $CDCl_3$; temperature: 20 °C; conversion determined by ^{1}H NMR; lines are intended as visual aids only.

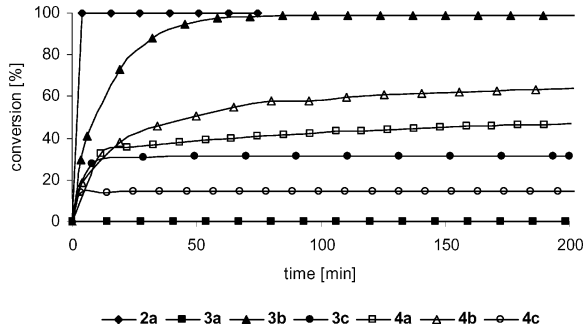

Figure 7. RCM of *N*,*N*-diallyltosylamide (**8**), catalysts **3a**–**c**, **4a**–**c**. Catalyst/substrate ratio 1:200; solvent: $CDCl_3$; temperature: 20 °C; conversion determined by ^{1}H NMR; lines are intended as visual aids only.

The results for the RCM of **6** using catalysts **2a**, **3a**–**c** and **4a**–**c** are depicted in Figure 5. The first-generation catalyst **2a** affords higher conversions at shorter reaction times compared to its second-generation counterparts **3a**–**b** and **4a**–**b**. Complexes **3c** and **4c**, containing a pyridine ligand, show high initial activity but activities drop dramatically after 0.5 h, pointing to their fast decomposition. The pyr-

idine ligand proves to stabilize the propagating species insufficiently during the RCM reaction. Surprisingly, the activity of **3c** reaches 40% compared to only 10% for catalyst **4c**, suggesting that the propagating species of **4c** is much more vulnerable to decomposition. In case of a PPh_3 ligand *trans* to the NHC ligand, high conversions are obtained after 3 h for **3b** and **4b**, respectively 96% and 85%.

In contrast to the complexes with a PPh_3 ligand, complexes with a stronger coordinating PCy_3 ligand exhibit a slower initiation. **3a** shows a conversion of 50% after 5 h for the RCM of **6**. However, the conversion proceeds to 89% after 24 h, which indicates a long lifetime of the complex. Full conversion could not be attained. **4a** exhibits the same behaviour but exceeds the activity of **3a**; after 24 h **4a** reaches quantitative conversion (>98%). At elevated temperatures, catalyst **4a** exceeds the activity of both catalyst **1c** and **3a**, the latter of which is the least reactive of the catalysts examined at higher temperatures (Figure 6). At lower temperatures, the need for ligand dissociation again proves to aggrieve PCy_3-ligand-containing catalysts, but gives rise to improved catalyst lifetimes of the catalysts.

The results for the RCM reaction of *N*,*N*-diallyltosylamide (**8**) using catalysts **2a**, **3a**–**c** and **4a**–**c** are given in Figure 7. Reaction proceeds smoothly using first-generation type catalyst **2a**, affording quantitative conversion within 4 min, a result that goes beyond the scope of all other catalysts reported. Catalyst **4a**, containing the SIMe ligand, shows a much better initial performance compared to **3a**, containing the SIMes ligand. The reactivity of the latter in RCM of **8** is very low with only 10% of conversion observed after 24 h at room temperature. Such strong effect of the SIMe ligand on performance has not been observed for catalysts **3b**–**c** and **4b**–**c**. The relatively small difference in substitution pattern between the discussed NHC ligands has a definite effect on the ligand dissociation of the PCy_3-ligand-containing catalysts.

Catalysts **3b** and **4b** are highly efficient toward the RCM of **8**; the former catalyzing the reaction much more efficiently than other second-generation-type catalysts, affording quantitative yields within 1 h. The activity of **4b** stagnates at 60% after 2 h. We presume that the lack of stability of the propagating species of the SIMe-ligand-containing catalyst impedes full conversion of the substrate.

As in the case of RCM of **6**, the pyridine-containing catalysts **3c** and **4c** exhibit a high initial activity ensued by an abrupt drop in activity. Again, the SIMes-containing catalysts show a higher conversion, supporting the conclusion that catalysts containing the SIMe ligand decompose more easily.

A better understanding of the different activities of the catalysts discussed can be achieved by determining the turnover numbers (TON's) at low catalyst loadings. Therefore, we tested the six catalysts in the RCM of *N*,*N*-diallyltosylamide **8** at 0.1 mol-% (Table 6). Under these conditions, the catalyst lifetime becomes extremely important, such that the indenylidene catalyst **3a**, which was almost completely impotent at room temperature, emerges as the most productive of the systems examined at elevated temperature.

Table 6. Performance of Ru-indenylidene catalysts **2a**, **3a**–**c** and **4a**–**c** in the RCM of **8**.[a]

Catalyst	TON at 20 °C	TON at 60 °C
2a	813	787
3a	170	970
3b	325	641
3c	110	114
4a	113	793
4b	191	546
4c	110	110

[a] Conditions: Catalyst/substrate ratio 1:1000, solvent: $CDCl_3$, conversion determined by ^1H NMR spectroscopy.

Where results for PCy_3-containing catalysts **3a** and **4a** are lower than their PPh_3-containing analogues **3b** and **4b** at 20 °C, they prove to be able to excel the activity of the latter at 60 °C. Upon heating to 60 °C, the activity of the first-generation catalyst **2a** drops slightly, due to a higher degree of decomposition. The pyridine-containing catalysts **3c** and **4c** again fail to deliver high TON's in RCM reactions, consistent with the results previously reported.

Schmidt and co-workers have proposed diallylsilane derivative **10** as a challenging substrate for RCM, since the large silicon atom disfavors the transition state geometry for cyclization reactions.[12] Table 7 (entries 1–7) show that PCy_3-ligand-containing second-generation catalysts (**3a**, **4a**, and **1c**) exhibit better performance towards the RCM of **10**, but high catalyst loadings (5 mol-%) remain vital. A literature report for **1c** (5 mol-%) describes only 70% formation of **11** after 16 h in CCl_4 at 65 °C,[12] compared to 76–95% for indenylidene catalysts **4a** and **3a** respectively. Catalyst **3a** excels all other catalysts, with nearly quantitative formation of **11** within 16 h in refluxing $CDCl_3$. PPh_3- and pyridine-containing catalysts **3b**, **4b**, **3c** and **4c** are less interesting catalysts regarding to this substrate. In addition, it should be noted that SIMes-containing catalysts are preferred to SIMe-containing catalysts for RCM of **10**. The reduced steric bulk of the phosphane ligand in **4a** compared to the SIMes ligand in **1c** and **3a** again plays a distinctive role in the higher reactivity of **3a** towards this substrate, and favors metathesis over deactivation.

A dissociative mechanism in which catalyst initiation depends upon phosphane dissociation is the most preferred for the olefin metathesis reactions catalyzed by Grubbs'[13,14] complexes **1a**–**c** and this also holds for indenylidene complexes. Therefore, it is undeniable that complexes containing SIMe ligand poses higher initiation efficiency than their mesityl analogues. As phosphane dissociation promotes catalyst decomposition, it is not surprising then that complexes bearing SIMe ligand decompose faster. The pyridine complexes **3c** and **4c** do not show a good catalytic activity when they are compared with the other catalysts. The pyridine ligand has weak electron donating properties and is not capable of stabilizing the active species formed in the metathesis reaction. This results in decomposition of the catalyst.

Cross Metathesis (CM) between two olefinic partners is an excellent way for the preparation of functionalized

Table 7. Representative Ring-Closing and Cross-Metathesis reactions.

Entry	Substrate	Product	Cat.	Catalyst loading [mol-%]	Time [h]	*T* [°C]	Solvent	% Conv./ *E*/*Z* ratio
1	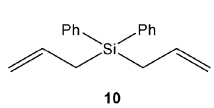 **10**	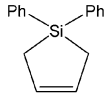 **11**	**1c**[a]	5	16	65	CCl_4	70
2			**3a**	5	16	60	$CDCl_3$	95
3			**3b**	5	2	60	$CDCl_3$	68
4			**3c**	5	2	60	$CDCl_3$	62
5			**4a**	5	2	60	$CDCl_3$	76
6			**4b**	5	2	60	$CDCl_3$	62
7			**4c**	5	2	60	$CDCl_3$	42
8	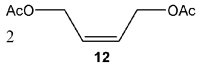 **12**	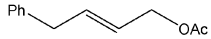 **14**	**1c**[b]	2.5	16	40	CD_2Cl_2	68/7.2
9			**3a**[b]	2.5	16	40	CD_2Cl_2	95/13.5
10			**3b**	2.5	2	40	CD_2Cl_2	63/7.4
11			**3c**	2.5	2	40	CD_2Cl_2	60/7.8
12	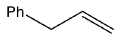 **13**		**4a**	2.5	2	40	CD_2Cl_2	67/5.8
13			**4b**	2.5	2	40	CD_2Cl_2	56/5.0
14			**4c**	2.5	2	40	CD_2Cl_2	40/4.5
15	 **15**	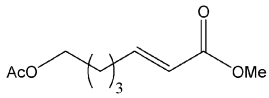 **17**	**1c**[c]	2.5	16	40	$CDCl_3$	55
16			**3a**	2.5	16	40	CD_2Cl_2	58
17			**3b**	2.5	3	40	CD_2Cl_2	35
18			**3c**	2.5	3	40	CD_2Cl_2	10
19	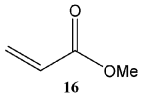 **16**		**4a**	2.5	3	40	CD_2Cl_2	40
20			**4b**	2.5	3	40	CD_2Cl_2	33
21			**4c**	2.5	3	40	CD_2Cl_2	2

alkenes and important building blocks for organic synthesis.[15] Results for the CM reaction between 1,4-diacetoxy-2-butene (**12**) and allylbenzene (**13**) are listed in Table 7, entries 8–14. Nearly quantitative transformation to **14** can only be achieved in the case of **3a**. The results of reactions conducted in CD_2Cl_2 at 40 °C, as compiled in Table 7, indicate that all other complexes tested were almost indistinguishable in terms of their activity. Most notably, however, SIMes-based precatalysts yield higher conversions for the hetero coupled product with higher *E*/*Z* selectivities; 7.4–13.5 for **1c**, **3a**–**c** and 4.5–5.8 for **4a**–**c**. The difference between the two catalyst classes can be rationalized on the basis of the greater stability of SIMes-containing catalysts and their ability to promote secondary metathesis, leading to the thermodynamically favored *E* isomer.[11]

Methyl acrylate (**16**) is a challenging substrate in olefin metathesis, and the Cross-Metathesis reaction with 5-hexenyl acetate (**15**) is a rather demanding reaction and therefore a better indicator for catalyst performance towards electron-deficient olefins. Results are shown in Table 7, entries 15–21. The difference between results obtained for SIMes- and SIMe-based precatalysts is not as discernible compared to the difference in results for the CM reaction of 1,4-diacetoxy-2-butene (**12**) and allylbenzene (**13**). Catalysts **1c** and **3a**, however, exhibit conversions excelling those obtained with other catalysts. In general, SIMes-containing catalysts give rise to higher conversions compared to their SIMe-containing analogues. The same trends in activity, as in the CM reactions described above, were observed. The third-generation indenylidene catalysts yield less than 10% of product. The only CM product observed is the *E* isomer, which is in agreement with the data presented in literature.[11]

Figure 8 displays the catalytic performance for ROMP of 1,5-cyclooctadiene (COD) (**18**) (Scheme 2) with a catalyst to monomer ratio of 1:3000.

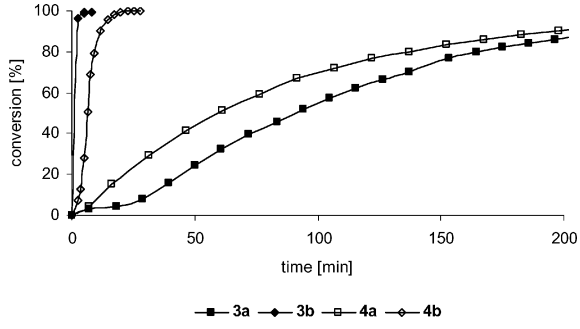

Figure 8. ROMP of 1,5-cyclooctadiene (**18**), catalysts **3a**–**b** and **4a**–**b**. Catalyst/monomer ratio 1:3000; solvent: $CDCl_3$; temperature: 20 °C; conversion determined by ^1H NMR; lines are intended as visual aids.

Third-generation indenylidene-Ru complexes **3c** and **4c** yield full monomer conversion within two minutes at a monomer-to-catalyst ratio of 1:3000, a performance far beyond that of the 2nd-generation indenylidene-Ru catalysts like **3a** and **4a**. Even though our 2nd-generation complexes with PPh_3 ligands **3b** and **4b** initiate ROMP slower than **3c** and **4c**, they still manage 100% conversion within 20 min. Quite rewardingly, at much lower catalyst loadings (10,000 equiv. of COD), **3c** and **4c** afford total monomer conversion within 15 min.

It has previously been described, that the polymerization of cyclooctadiene (COD) is initially not stereoselective.[16a] Since only one double bond of *cis*,*cis*-COD is opened, a 75:25 *cis*/*trans* ratio represents the theoretically predicted

non-selective polymerization. Although ofefin metathesis catalysts show no preference for the *trans*-orientation in the initial stage of the COD polymerization, a secondary metathesis event transforms the polymer into a polymer with higher *trans* content.[16b] Moreover, when sufficient *trans*-polymer has been produced by secondary metathesis, a tertiary metathesis event occurs, which transforms *trans*-1,4-polybutadiene into *t*,*t*,*t*-1,5,9-cyclododecatriene, **20** (CDT) (Scheme 3, Table 8).[16b]

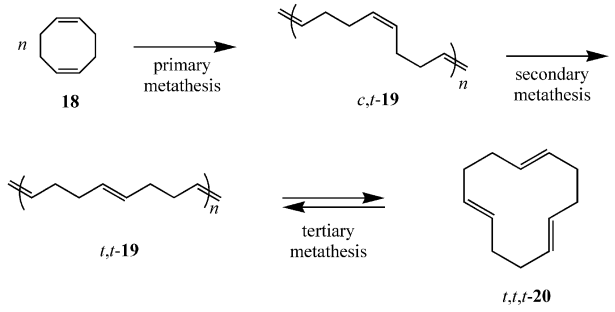

Scheme 3. Formation of CDT (**20**) during the ROMP of COD (**18**).

Table 8. Formation of CDT (**20**) during the ROMP of COD (**18**).[a]

Catalyst	*T* [°C]	Time [h]	*cis* [%][b]	CDT [%]	TON
1c	25	24	54	0	2900
3a	25	24	75	0	3000
3b	25	0.3	17	4.7	3000
3c	25	0.25	8	10	10000
4a	25	24	75	0	3000
4b	25	0.3	20	1	3000
4c	25	0.25	9	10	10000

[a] Conditions: catalyst concentration 0.453 mM, solvent $CDCl_3$, *T* = 20 °C, conversion determined by ^1H NMR spectroscopy. [b] Percentage of olefin with *cis* configuration in the polymer backbone; ratio based on data from ^1H and ^{13}C NMR spectra (^{13}C NMR spectroscopy: δ = 32.9 ppm allylic carbon *trans*; δ = 27.6 ppm allylic carbon *cis*).

Transformation of the 1,4-polybutadiene chain into *t*,*t*,*t*-CDT is not observed in case of catalysts **3a**, **4a** and **1c** (Scheme 3). Contrary to the indenylidene-type catalysts **3a** and **4a**, catalyst **1c** exhibits moderate secondary metathesis activity as reflected by the higher *trans*-content.

Catalysts **3b**–**c** and **4b**–**c** yield high conversions in very short reaction times accompanied by high percentages of *trans*-polymer, a result of their excellent initiation and propagation rates. The high performance of these catalysts further allowed tertiary metathesis to occur transforming the *trans*-1,4-polybutadiene into *t*,*t*,*t*-CDT.

Conclusions

In this article, we presented the synthesis of and catalytic data for a series of second- and third-generation indenylidene ruthenium catalysts applied to a set of standard olefin metathesis transformations. The aim of this study was to reveal the relative efficacies of different catalysts containing a SIMes or a SIMe ligand. We have compared six of the indenylidene ruthenium olefin metathesis catalysts in a set of metathesis reactions and described them in terms of their performance, selectivity, and stability. It was evidenced that a small modification of the substituents on the NHC ligand influences the catalyst initiation rate. Nevertheless, as facile ligand (phosphane, pyridine) dissociation often preceeds catalyst decomposition, complexes bearing a SIMe ligand decompose faster. Although there is no single best catalyst available, for all metathesis transformation, the reactivity trends in CM were found to be similar to those observed in RCM. Furthermore, higher selectivities were found for SIMes-containing catalysts in the CM of allylbenzene with 1,4-diacetoxy-2-butene **12**. Nearly quantitative transformation to the reaction product has been observed using **3a** in RCM of *N*,*N*-diallyltosylamide **8** at low catalysts loadings (0.1 mol-%) and the sterically demanding diphenyl diallylsilane **10** and CM of allylbenzene with 1,4-diacetoxy-2-butene **12**. However, its low initiation efficiency at room temperature, **3a** frequently excels other catalysts in RCM and CM reactions. The efficiency of **3c** and **4c** for ring-opening metathesis polymerization of 1,5-cyclooctadiene is remarkable, affording complete conversion at very low catalyst loadings within 2 min. As a high initiation rate is a requisite for this type of reaction, the second-generation indenylidene **3a**, **4a** catalysts are dramatically less active in this transformation. For catalysts **3a** and **4a** an induction period was observed after which the reaction follows pseudo-first-order kinetics. Additionally, evidence was found for secondary and tertiary metathesis reactions in case catalysts **3b**,**c** and **4b**,**c** were used for ROMP of COD, different from classical second-generation catalysts **3a** and **4a**.

Complete resonance assignment of all complexes studied is shown to be relatively straightforward, and should be easily extendable to other such complexes, especially since the extensive ring currents in one or more ligands confer favorable dispersion in the ^1H NMR spectrum. The assignment affords the characterization of various conformational processes and the possible influences of the ligand there upon. Given the small set of molecules characterized so far, and the fact that several effects can simultaneously contribute to the chemical shift, the investigation of correlations with the catalytic performance are currently beyond reach. Keeping in mind that the chemical shift information is relevant to the initial state of the catalyst only, the confrontation of chemical shift and conformational information collected using NMR with catalytic performance may become of interest when a sufficiently large number of well considered complexes have been fully characterized.

Experimental Section

General: Reactions were performed under inert argon atmosphere using the Schlenk technique. Argon was dried by passage through drierite. Solvents like tetrahydrofuran (THF), toluene, dichloromethane (DCM), hexane, [D_6]benzene, [D]chloroform were dried by standard methods and degassed by a standard three freeze-pump-thaw cycles. Methanol was not dried before use. Pyridine was nor dried nor degassed before use. Diethyl diallylmalonate was purchased from Aldrich and used as received. Complexes **2a**,**b**[7] and **3a**–**c**[6] were synthesized as described before in the literature.

1D and 2D ^1H, ^{13}C and ^{31}P NMR spectra were recorded on either a Bruker Avance 300 MHz spectrometer (for ^{31}P only using a 5 mm BBO probe), Bruker DRX 500 MHz spectrometer (5 mm TXI probe) and a Bruker Avance II 700 MHz NMR spectrometer (5 mm TXI probe). The latter was mainly used to validate assignments made at 500 MHz that were ambiguous due to insufficient resolution. ROESY spectra were recorded using the off-resonance scheme with an angle of 60°.[17] Chemical shift values (δ) are given in parts per million (ppm) using the residual C_6D_5H as secondary internal calibration reference. For ^{31}P, H_3PO_4 was used as external reference. All kinetic experiments were performed on a Varian Unity 300 MHz spectrometer.

(SIMe)(PCy_3)Cl_2Ru(3-phenylindenylid-1-ene) (4a): A flame-dried reaction flask is charged with 286.0 mg (0.3098 mmol) of compound **2a** and 159.3 mg (0.3568 mmol; 1.15 equiv.) of the pentafluorobenzene adduct **5b**. The mixture is dissolved in 10 mL of toluene, stirred and heated to 100 °C for 1.5 h. The reaction mixture is cooled down to room temperature and filtered off. All volatiles are removed by evaporation and the residue is suspended in 5 mL of MeOH. After filtration, the residue is washed with another 5 mL of MeOH and dried in vacuo to afford 160.5 mg (0.1743 mmol; 56%) of **4a** as a red powder. The NMR spectroscopic data is available in Tables 1 and 2 in the main text.

(SIMe)(PPh_3)Cl_2Ru(3-phenylindenylid-1-ene) (4b). Method A: Under an inert atmosphere of Ar, 35.1 mg PPh_3 (0.134 mmol; 1.10 equiv.) is added to 87.3 mg **4c** (0.121 mmol) in dichloromethane (10 mL) and the mixture is stirred for 30 min at room temperature. After evaporation of all volatiles, the residue is suspended in *n*-hexane and filtered off. Thoroughly washing with 3 × 5 mL *n*-hexane and drying in vacuo yielded 57.7 mg of **4b** (0.064 mmol; 53%) as a deep red powder.

Method B: Under an inert atmosphere of Ar, a flame-dried reaction flask is charged with 275.3 mg (0.3105 mmol) of complex **2b** and 159.4 mg (0.3571 mmol; 1.15 equiv.) of the pentafluorobenzene adduct **5b**. The mixture is dissolved in 10 mL of toluene, stirred and heated to 100 °C for 1 h. The reaction mixture is cooled down to room temperature and filtered off. All volatiles are removed by evaporation and the residue is suspended in 5 mL of MeOH. After filtration, the residue is washed with another 5 mL of MeOH and dried in vacuo to afford 211.7 mg (0.2299 mmol; 74%) of **4b**. The NMR spectroscopic data is available in Table 1 and in the main text.

(SIMe)(py)Cl_2Ru(3-phenylindenylid-1-ene) 4c: 152.0 mg (0.165 mmol) of complex **4a** is dissolved in pyridine (2.0 mL) and stirred at room temperature for 2 h. A brown precipitate is formed upon addition of n-hexane (10 mL) and subsequent cooling to –40 °C. Filtration of the precipitate, washing with 3 × 5 mL n-hexane and drying in vacuo yielded 87.3 mg (0.121 mmol; 73%) of compound **4c** as an orange powder. The NMR spectroscopic data is available in Tables 1 and 3 in the main text.

Monitoring ROMP of *cis*,*cis*-Cycloocta-1,5-diene (COD, 18): An NMR tube is charged with the appropriate amount of catalyst, dissolved in 0.60 mL of $CDCl_3$. 0.10 mL of *cis*,*cis*-cycloocta-1,5-diene is added, the NMR tube is closed and the conversion is determined by integration of the olefinic ^1H signals of the formed polymer and the consumed monomer.

Monitoring RCM of Diethyl Diallylmalonate (6) and *N*,*N*-Diallyltosylamide (8): An NMR tube is charged with the appropriate amount of catalyst, dissolved in 0.60 mL of $CDCl_3$. Next 0.10 mL of the substrate is added, the NMR tube is closed and the conversion is determined by integration of the allylic ^1H signals of the formed product and the consumed substrate.

Acknowledgments

R. D. and F. V. thank Ralf Karch and Roland Winde of UMICORE AG for a generous gift of Neolyst M1 and Neolyst M2. The IWT Flanders is thanked for a PhD grant to P. M. S. H. J. C. M. and F. V. thank the FWO for financial support and several NMR equipment grants (G.0036.00N, G.0365.03). The 700 MHz equipment of the Interuniversitary NMR Facility was financed by Ghent University, the Free University of Brussels (VUB) and the University of Antwerp via the "Zware Apparatuur" Incentive of the Flemish Government. S. M. and F. V. gratefully acknowledge the Research Fund of Ghent University (BOF) for the financial support.

[1] For selected reviews on olefin metathesis, see a) T. M. Trnka, R. H. Grubbs, *Acc. Chem. Res.* **2001**, *34*, 18–29; b) R. H. Grubbs, *Handbook of Metathesis*, Wiley-VCH, Weinheim (Germany), **2003**; c) S. J. Connon, S. Blechert, *Angew. Chem.* **2003**, *115*, 1944–1968; d) D. Astruc, *New J. Chem.* **2005**, *29*, 42–56.

[2] a) P. Schwab, M. B. France, J. W. Ziller, R. H. Grubbs, *Angew. Chem. Int. Ed. Engl.* **1995**, *34*, 2039–2041; b) P. Schwab, R. H. Grubbs, J. W. Ziller, *J. Am. Chem. Soc.* **1996**, *118*, 100–110; c) M. Scholl, T. M. Trnka, J. P. Morgan, R. H. Grubbs, *Tetrahedron Lett.* **1999**, *40*, 2247–2250; d) T. Weskamp, W. C. Schattenmann, M. Spiegler, W. A. Herrmann, *Angew. Chem. Int. Ed.* **1998**, *37*, 2490–2493; e) M. S. Sanford, J. A. Love, R. H. Grubbs, *Organometallics* **2001**, *20*, 5314–5318; f) J. Huang, E. D. Stevens, S. P. Nolan, J. L. Peterson, *J. Am. Chem. Soc.* **1999**, *121*, 2674–2678; g) J. Huang, H.-J. Schanz, E. D. Stevens, S. P. Nolan, *Organometallics* **1999**, *18*, 5375–5380; h) J. C. Conrad, G. P. A. Yap, D. E. Fogg, *Organometallics* **2003**, *22*, 1986–1988; i) T. M. Trnka, J. P. Morgan, M. S. Sanford, T. E. Wilhelm, M. Scholl, T.-L. Choi, S. Ding, M. W. Day, R. H. Grubbs, *J. Am. Chem. Soc.* **2003**, *125*, 2546–2558.

[3] a) J. S. Kingsbury, J. P. A. Harrity, P. J. Bonitatebus, A. H. Hoveyda, *J. Am. Chem. Soc.* **1999**, *121*, 791–799; b) S. B. Garber, J. S. Kingsbury, B. L. Gray, A. H. Hoveyda, *J. Am. Chem. Soc.* **2000**, *122*, 8168–8179.

[4] a) R. Bujok, M. Bieniek, M. Masnyk, A. Michrowska, A. Sarosiek, H. Stepowska, D. Arlt, K. Grela, *J. Org. Chem.* **2004**, *69*, 6894–6896; b) A. Michrowksa, R. Bujok, S. Harutyunyan, V. Sashuk, G. Dolgonos, K. Grela, *J. Am. Chem. Soc.* **2004**, *126*, 9318–9325.

[5] a) S. Gessler, S. Randl, S. Blechert, *Tetrahedron Lett.* **2000**, *41*, 9973–9976; b) H. Wakamatsu, S. Blechert, *Angew. Chem. Int. Ed.* **2002**, *41*, 2403–2405; c) H. Wakamatsu, S. Blechert, *Angew. Chem. Int. Ed.* **2002**, *41*, 794–796.

[6] S. Monsaert, R. Drozdzak, V. Dragutan, I. Dragutan, F. Verpoort, *Eur. J. Inorg. Chem.* **2008**, *3*, 432–440.

[7] a) L. Jafarpour, H.-J. Schanz, E. D. Stevens, S. P. Nolan, *Organometallics* **1999**, *18*, 5416–5419; b) A. Fürstner, O. Guth, A. Düffels, G. Seidel, M. Liebl, B. Gabor, R. Mynott, *Chem. Eur. J.* **2001**, *7*, 4811–4820; c) E. A. Shaffer, C.-L. Chen, A. M. Beatty, E. J. Valente, H.-J. Schanz, *J. Organomet. Chem.* **2007**, *692*, 5221–5233.

[8] H. Clavier, S. P. Nolan, *Chem. Eur. J.* **2007**, *13*, 8029–8036.

[9] I. C. Stewart, T. Ung, A. A. Pletnev, J. M. Berlin, R. H. Grubbs, Y. Schrodi, *Org. Lett.* **2007**, *9*, 1589–1592.

[10] a) T. M. Trnka, E. L. Dias, M. W. Day, R. H. Grubbs, *ARKIVOC* **2002**, *13*, 28–41; b) H. Clavier, J. L. Petersen, S. P. Nolan, *J. Organomet. Chem.* **2006**, *691*, 5444–5447.

[11] T. Ritter, A. Hejl, A. G. Wenzel, T. W. Funk, R. H. Grubbs, *Organometallics* **2006**, *25*, 5740–5745.

[12] B. Schmidt, M. Pohler, B. Costisella, *J. Org. Chem.* **2004**, *69*, 1421–1424.

[13] M. S. Sanford, J. A. Love, R. H. Grubbs, *J. Am. Chem. Soc.* **2001**, *123*, 6543–6554.

[14] W. J. van Rensburg, P. J. Steynberg, W. H. Meyer, M. M. Kirk, G. S. Forman, *J. Am. Chem. Soc.* **2004**, *126*, 14332–14333.
[15] a) A. K. Chatterjee, R. H. Grubbs, *Org. Lett.* **1999**, *1*, 1751–1753; b) A. K. Chatterjee, J. P. Morgan, M. Scholl, R. H. Grubbs, *J. Am. Chem. Soc.* **2000**, *122*, 3783–3784; c) T.-L. Choi, C. W. Lee, A. K. Chatterjee, R. H. Grubbs, *J. Am. Chem. Soc.* **2001**, *123*, 10417–10418; d) D. Bourgeois, A. Pancrazi, S. P. Nolan, J. Prunet, *J. Organomet. Chem.* **2002**, *643–644*, 247–252; e) S. D. Goldberg, R. H. Grubbs, *Angew. Chem. Int. Ed.* **2002**, *41*, 807–810; f) A. K. Chatterjee, R. H. Grubbs, *Angew. Chem. Int. Ed.* **2002**, *41*, 3171–3174; g) A. K. Chatterjee, T.-L. Choi, D. P. Sanders, R. H. Grubbs, *J. Am. Chem. Soc.* **2003**, *125*, 11360–11370.
[16] a) E. Thorn-Csányi, K. Ruhland, *Macromol. Chem. Phys.* **1999**, *200*, 1662–1671; b) B. Allaert, N. Ledoux, N. Dieltens, H. Van der Mierde, C. V. Stevens, P. Van Der Voort, F. Verpoort, *Catal. Commun.* **2008**, *9*, 1054–1059.
[17] a) H. Desvaux, P. Berthault, N. Birlirakis, M. Goldman, *J. Magn. Reson.* **1994**, *108*, 219–229; b) N. Birlirakis, P. Berthault, H. Desvaux, M. Goldman, *Bruker Report* **1996**, *142*, 34–38.

Received: October 3, 2008
Published Online: December 19, 2008

